Original scientific paper

UDC: 655.36:004.9
778

Investigation of the accuracy of close-range photogrammetry – a 3D printing case study

ABSTRACT

3D scanning of physical objects is one of the frequently used methods for generating input data for 3D printing process. Close-range photogrammetry represents a cost-efficient alternative to conventional 3D scanning. However, one of the basic problems in application of this method is accuracy, especially in the case of small objects with complex geometry. In this case study, a 3D-printed object of small dimensions was used to test the accuracy and precision of close-range photogrammetry. CAD Inspection was used to obtain measurements of the scanned model and compare it with the original CAD model, while the results were statistically analyzed. The results of statistical analysis showed that the scanning accuracy in this experiment did not depend on the particular cross-section of the model, while the precision of 3D scanning depended on the selection of cross-sectional profile curve.

KEY WORDS

3D printing, Fused deposition modeling, close-range photogrammetry, CAD inspection, accuracy.

Ognjan Lužanin[1], Irma Puškarević[2]

[1]*University of Novi Sad, Faculty of Technical Sciences, Department of Production Engineering, Novi Sad*
[2]*University of Novi Sad, Faculty of Technical Sciences, Department of Graphic Engineering and Design, Novi Sad*

Corresponding author:
Ognjan Lužanin
e-mail: luzanin@uns.ac.rs

First recieved: 18.06.2015.
Accepted: 21.07.2015.

Introduction

Although most popular, CAD modelling is not the only method which can be used to generate input data for 3D printing processes (Gibson et al, 2010). 3D scanning is also often used to acquire 3D digital models based on physical originals. In the recent years, the constant advancement of hardware and software applications, allowed the spread of photography-based reconstructive procedures. In the available literature as well as on the Internet, this particular method appears under several designations, of which most frequently used are: Photo-based 3D scanning, Structure-from-Motion /SfM/ and Close-Range Photogrammetry (Mitchell, 2007).

Due to its popularity, 3D scanning based on photography is now employed by various professions, ranging from archeologists, to terrain surveyors, architects and art conservationists to forensics. With this in mind, 3D close-range photogrammetry scanning represents an interesting research topic, especially regarding the issue of geometric accuracy. Although one does not expect the geometric accuracy of this method to match that of the professional 3D scanners, it is very interesting to examine the scale and configuration of errors, as well as to assess whether this affordable scanning method can be applied with success in numerous cases when high accuracy is not of primary concern.

In this study, close-range photogrammetry was used to obtain a surface model of a 3D-printed small-size figure, using a commercial 3D scanning software. Thus obtained, the 3D scan was imported into a CAI (Computer Aided Inspection) software and compared with the original CAD master file. Dimensional deviations were sampled and statistically analyzed on two pre-selected characteristic profile curves to examine the differences in accuracy and precision as the function of model geometry. With this in mind, the paper is organized as follows: Section 2 presents a short introduction to close-range photogrammetry and its basic principle of operation; covered in Section 3 are the main stages of this case-study, from 3D printing of the scanning model, to image acquisition, to image processing and surface

model generation; details of CAI inspection are given in Section 4, followed by the statistical analysis of results in Section 5; concluding remarks are presented in Section 6, while Section 7 contains a list of references.

Close-range photogrammetry

For lack of a universally accepted definition, there are several popular interpretations of photogrammetry. For instance, the American Society for Photogrammetry and Remote Sensing (ASPRS) defines the photogrammetry as the skill, science and technology aimed at providing reliable information on physical objects and environment, through recording measuring and interpretation of photo images, as well as the images of EM radiation and other phenomena (ASPRS, 2008). Schenk (Schenk, 2005) also gives a popular definition of photogrammetry stating that photogrammetry is the science of obtaining reliable information about the properties of surfaces and objects without physical contact with the objects, and of measuring and interpreting this information.

Regardless of the definition, photogrammetry employs methods from various disciplines, including optics and projective geometry (Luhmann, 2010). The term "photogrammetry" stems from the following Greek words; photos meaning light, gramma meaning to draw, and metron meaning to measure (Awange & Kiema, 2013).

Notes from the history of photogrammetry

Photogrammetry dates back to mid-nineteenth century, while its origins are related to a French officer, Aime Laussedat, who is attributed with the development of the first photogrammetric devices and methods, in 1851. Another distinguished year for the development of photogrammetry was 1858, when the German architect A. Meydenbauer developed photogrammetric techniques for the documentation of buildings. In addition, the first photogrammetric institution, the Royal Prussian Photogrammetric Institute, was established in 1885. That same year is also related to the first successful large-scale application of photogrammetry- the photogrammetric recording of the ancient ruins of Persepolis.

Modern photogrammetry saw its expansion during the mid-eighties of the twentieth century, thanks to the rapid development and improvement of PC computers and software.

Principle of operation

The usual workflow includes taking pictures (nowadays digital cameras are predominant) from various view perspectives with partial overlap (Figure 1). Shown in Figure 1 are four digital cameras, i.e., their image chips, represented schematically by four plates (a). Projecting from the camera are light rays (b) which form spatial intersections and are projected onto various points on the object being scanned (c). Each camera lens has its focal point which is designated by a dot (d).

In the second phase, the taken images are imported into a specialized commercial or experimental software for close-range photogrammetry where the process called bundle triangulation takes place in an automated mode, resulting in the generation of 3D points coordinates. In-depth explanations of the principles of photogrammetry can be found in (Bösemann, 2005), (Awange & Kiema, 2013) and (Mitchell, 2007).

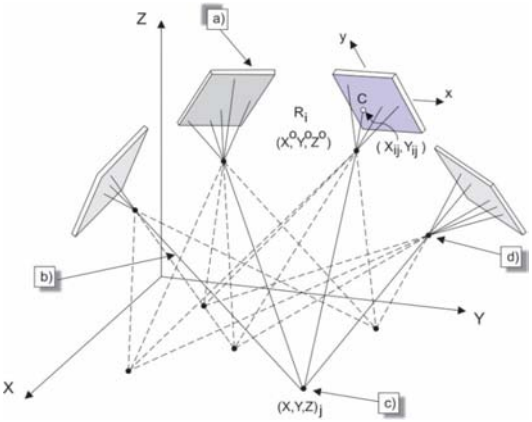

» **Figure 1:** *Principle schema of close-range photogrammetric process*

Case study - 3D scanning of a small-size 3D printed object

3D printing of the object

The physical model used in this study as the measuring object, was 3D printed on Makerbot Replicator 2, which uses Fused Deposition Modeling (FDM) technology. The original master digital model was in STEP format (Figure 2a) and was downloaded from http://www.grabcad.com. Upon download, the master model was converted into STL format (Figure 2b), imported into MakerWare software and prepared for 3D printing. Finally, the model was 3D printed using the settings given in Table 1. Completed model is shown in Figure 3.

Table 1

Working parameters used to 3D print the physical model used in experiment

Parameter	Value
Layer thickness	0.3 mm
Extrusion temperature	235 oC
Extrusion speed	80 mm/s
Infill	10 %

Generation of photo images of the 3D printed physical model

Tone value increase was also measured, they were determined using the Murray-Davis formula which is based on optical density data. We found no considerable changes in the TVI values during the experiment, the most affected was the black process colour with both substrates.

Photo images required for the close-range photogrammetry were acquired in an improvised studio, using following equipment:

- Photo camera (Canon EOS 1100D);
- Camera tripod;
- Studio flash;
- Reflector panel (Visico RD).

The setup is shown in Figure 4. To minimize the presence of shadow and allow efficient masking in the subsequent phase, white cardboard backdrop was used. The physical object was placed on an improvised platform which was custom-made of cardboard. A calibration mat with special markings- used by the software to determine the angle from which each photograph was taken- was placed on top of the platform. During experiment, the physical object was rested some 5 cm above the mat, to prevent occlusion of the dot markings.

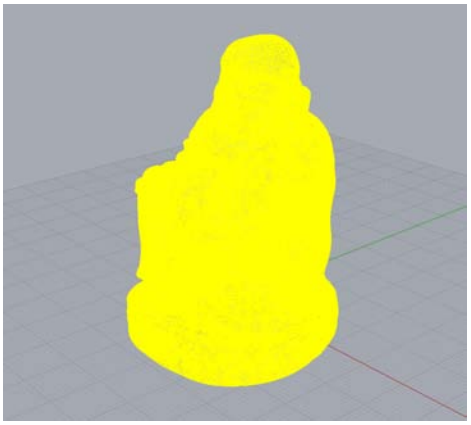

a)

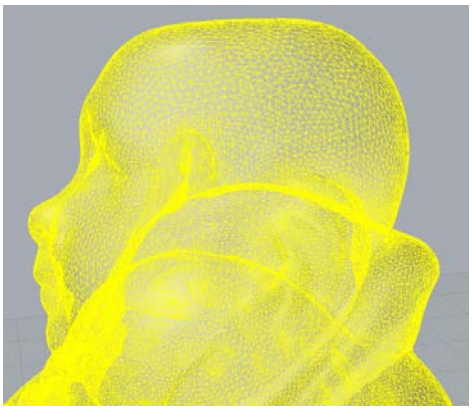

b)

» **Figure 2:** *STL model before export, a) entire model, b) detail of the head showing triangulated mesh*

» **Figure 3:** *Physical model on the printing plate after completion of the 3D printing process*

» **Figure 4:** *Setup used in the generation of photogrammetric images*

Processing of photo-images

A total of 21 photos were taken, of which 15 photos represent frontal perspective (Figure 5), 5 were taken from the three-quarter perspective, while the last photo represents birds-eye view. As shown in the setup image (Figure 4), the camera was fixed during the shooting, allowing the distance between the lens and the physical object to remain constant. Each of the 15 photos taken from the frontal perspective differed by the angular orientation of the physical object which was incrementally rotated according to indexing on the mat. The additional 5 three-quarter perspective shots were also taken from different angles.

Once the photo shoot was finished, calibration shots and the rest of the photos were transferred onto a PC computer with the installation of 3D Som Pro (3DSOM, 2014). In the following process, the photos were masked in an automated mode, after which the majority of photos were manually edited for mask correction.

Processing of scanned 3D model

Upon completion of the photo processing stage, the 3D model was generated in two additional stages:

1. Generation of the initial surface model;
2. Optimization of the generated model.

Within the second stage, the optimization was performed by defining the following three parameters: (i) number of silhouettes to be used for optimization (all silhouettes were selected, based on 21 photos); (ii) accuracy of approximation (maximum accuracy was avoided since, during previous attempts, it rendered an overly faceted model surface); (iii) point cloud was not used for optimization, considering the fact that the model surface was more even with this option off.

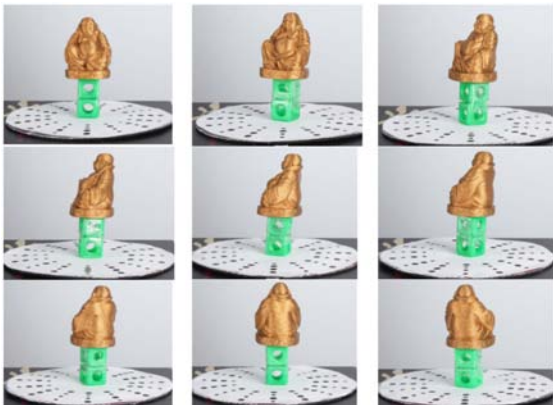

» **Figure 5:** *Photo shots ((9 out of 15) taken form the portray perspective based on the angular indexing*

The resulting models are shown in Figure 6 a-b. Figure 6a shows the model upon completion of the first stage, where the result is the initial surface model. Shown in Figure 6b is the optimized model.

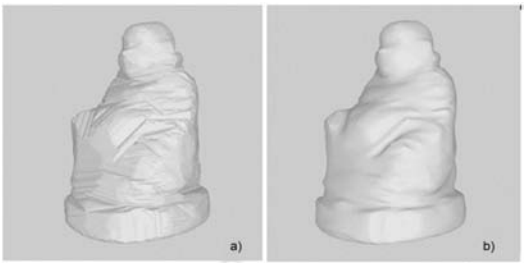

» **Figure 6:** *3D model generation shown in stages– a) the result of the first stage, b) the result of optimization*

Cad inspection (CAI) of the scanned 3d model

In this stage, the CAD master model and the scanned 3D model were imported into CAI software application, GOM Inspect (Gom Inspect, 2013). In the next stage, the two imported models were aligned, as required by the regular inspection procedure.

The generated diagnostic image showing deviations between the two models is shown in Figure 7.

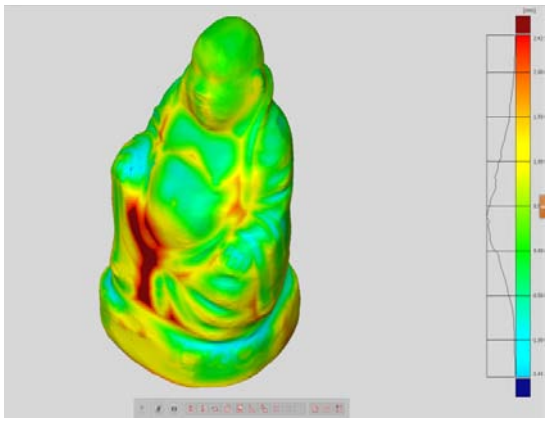

» **Figure 7:** *Scanned model with the superimposed color map with the deviations in ISO orientation*

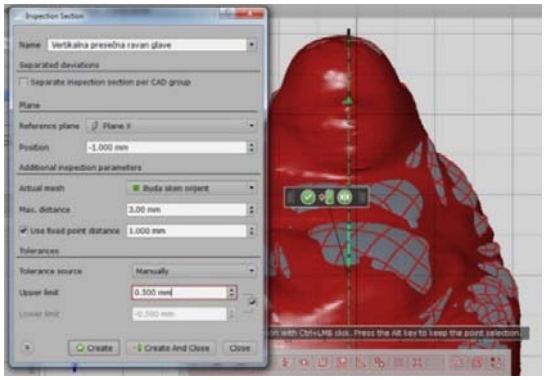

a)

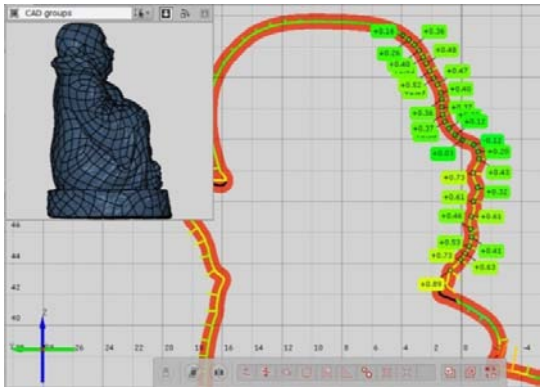

b)

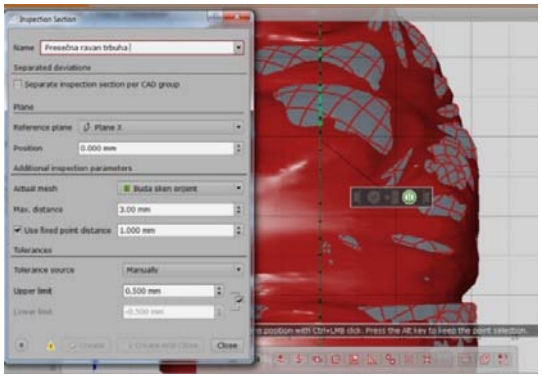

c)

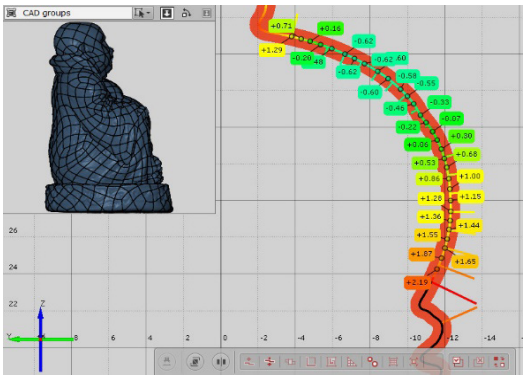

d)

» **Figure 8:** *Data acquisition in the CAI software - a) cross-sectional plane through the head, b) the resulting Head profile curve and 30 measuring points, c) cross-sectional plane through the belly, d) the resulting Belly profile curve and 30 measuring points*

Once the diagnostic image was generated, two cross-sectional planes were defined on the models – Head cross-section (Figure 8a) and Belly cross-section (Figure 8c). The two planes allowed the generation of two profile curves which were used for the sampling of measuring points- thirty points each. For each point a label was generated showing the measured deviation between the scanned 3D model and the reference CAD model (Figure 8b and Figure 8d).

Reproducible colour gamut is a useful indicator of print quality. The range of reproducible colours can be calculated by sampling the colour solid (gamut) obtained for a standard colour management profile.

Analysis of measurement results

In order to compare the deviations measured in two different cross-sections of the model- head and belly, an independent t-test was conducted. Statistical analysis was performed in Minitab v16. Based on the results of the Anderson-Darling normality test ($p<0.05$) there follows that the measurement results obtained for the belly profile curve, do not come from the normal distribution. Following the results of the Levene test for homogeneity of variances, $F(1,58)=55.11$, $p=.000$, hypothesis of homogeneity of variances was rejected. For that reason, Welch t-test was used since it does not assume equality of variances. Based on the Welch t-test, $t(32)=-0.01$, $p=.991$, it was concluded that the assumption about the differences in mean values of deviations on the Head profile curve ($M=0.406$, $SD=0.213$) and Belly profile curve ($M=0.404$, $SD=0.897$), cannot be rejected. Therefore, there was no statistically significant difference in accuracies of the scanning for the two profile curves. Boxplot diagrams (Figure 9a) indicate that the means of the two samples are very close, while the dispersions are evidently different, as shown in Figure 9b.

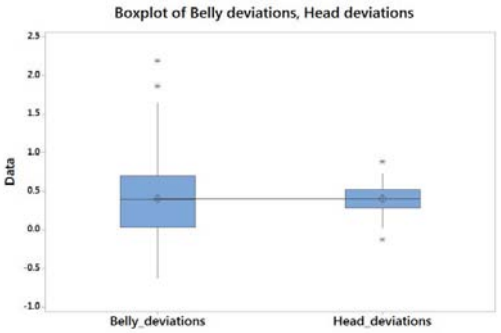

a)

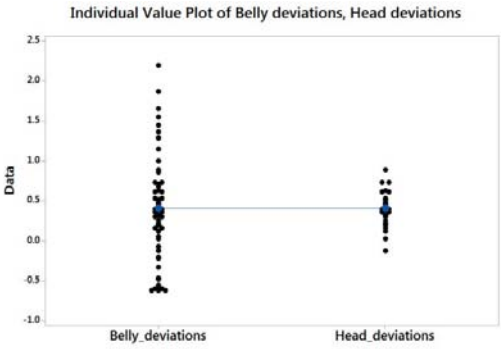

b)

» **Figure 9:** *Boxplots (a) and individual values plots (b) for the two samples of measuring points sampled on the Head and Belly profile curves*

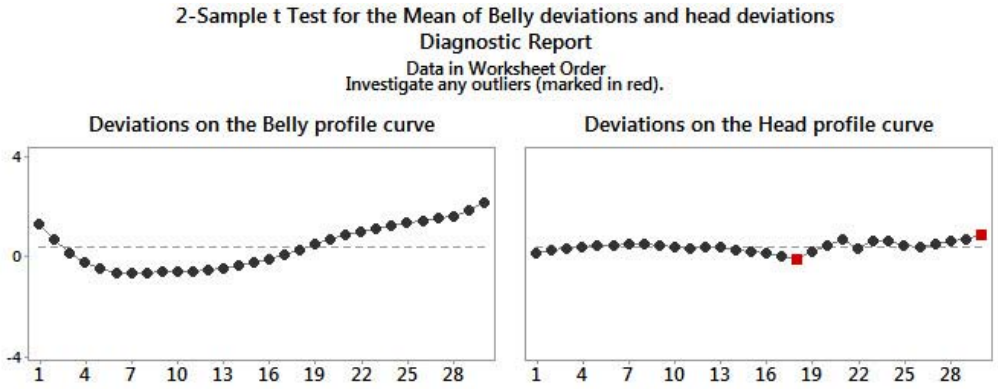

» **Figure 10:** *Deviations on the Belly and Head profile curves in the sampling order (outliers shown in red)*

Variance of the sample obtained on the Belly profile curve is significantly greater than that on the Head profile curve. Shown in Figure 10 is the diagram with the thirty sampled points for both profile curves, where the order of the deviations corresponds to the sampling order of the points. Evidently, there are two distinctive areas on the Belly profile curve, which contain either negative or positive deviations (Figure 10a). Such trend is not present in Figure 10b, which features two outliers shown in red.

Conclusion

In this case study, an experiment was conducted to assess the accuracy of 3D scanning based on close-range photogrammetry, using a complex-geometry 3D-printed model of small dimensions and a commercial software solution. The goal was to determine if there exist any differences in scanning accuracy and precision based on model geometry, i.e., in certain cross-sections. The deviation maps showed that the majority of deviations fall within the ±0.5 mm range, while the extreme deviations of 2.5 mm were observed in the zones with shallow relief details which are difficult to catch using this method, considering the small dimensions of the physical model. In order to test the differences in accuracy and precision of scanning as the function of model geometry, two cross-sectional planes were used to generate profile curves. Thirty measurement points were sampled on each generated profile curve in a random manner and the hypotheses of equal means and variances were tested using Welch t-test.
The results of statistical analysis showed that there is no statistically significant difference in means for the two samples, which indicates that the scanning accuracy in this experiment did not depend on the particular cross-section of the model. On the other hand, there was a statistically significant difference in variances of the two samples. Based on this, it can be concluded that, in this experiment, the precision of 3D scanning depended on the selection of cross-sectional profile curve.
As regards further investigation, the accuracy and precision of close-range photogrammetry scanning of small-size figures with complex geometry could be improved in following ways: (i) by reducing the surface glitter of the model which affects the quality of images, (ii) projection of a matrix of parallel lines onto the physical model during photo shoot, in order to increase accuracy and precision of scanning in the areas containing shallow relief and complex geometry, and (iii) improvement of camera calibration process, which greatly impacts the quality of central projection.

Acknowledgment

The results presented in this paper were obtained in the framework of the project “Research and development of modelling methods and approaches in manufacturing of dental recoveries with the application of modern technologies and computer aided systems” TR 35020, financed by the Ministry of Education, Science and Technological Development of the Republic of Serbia.

References

1. ASPRS (2008) ASPRS procurement guidelines committee. Guidelines for procurement of professional aerial imagery, photogrammetry, LiDAR and related remote sensor-based geospatial mapping services. Photogrammetric Engineering and Remote Sensing, Vol. 74. pp. 1286-1295.
2. Awange, J.L., Kyalo Kiema, J.B. (2013) Fundamentals of Photogrammetry. Environmental Geoinformatics Environmental Science and Engineering, Springer Berlin Heidelberg, pp. 157-174
3. Bösemann, W. (2005) Advances in Photogrammetric Measurement Solutions. Computers in Industry, 56 (8-9), pp.886-893.
4. Gibson, I., Rosen, D.W., Stucker, B. (2010) Additive manufacturing technologies. New York, Springer.
5. GOM Inspect (2013), Inspection V7.5 SR12, Manual-Basic. [Online] Available from: https://support.gom.com/display/DOCS/ [Accessed 12th May, 2015]
6. Luhmann, T. (2010) Close-Range Photogrammetry for Industrial Applications. ISPRS Journal of Photogrammetry and Remote Sensing, 65 (6), pp.558-569.
7. Mitchell, H.L (2007) Fundamentals of photogrammetry, Applications of 3D Measurements from Images, Whittles Publishing, Dunbeath, Scotland.
8. Schenk, T. (2005) Introduction to Photogrammetry. Department of Civil and Environmental Engineering and Geodetic Science, The Ohio State University, pp.79–95. [Online] Available from: http://gscphoto.ceegs.ohio-state.edu/courses/GeodSci410/docs/GS410_02.pdf. [Accessed Jan.21, 2015]
9. 3DSOM (2014) 3DSOM pro user guide. [Online] Available from: http://www.3dsom.com [Accessed 5th October, 2014]